

AN ACCURATE AND EXPLICIT PHYSICAL MODEL OF THE MOS TRANSISTOR

A.L.A. CUNHA, R.T. GONÇALVES, M.C. SCHNEIDER and C.G. MONTORO

LINSE / EEL / UFSC

Caixa Postal 476 - Florianópolis - CEP 88010-970 SC - Brasil

e-mail: LINSE@BRUFSC.BITNET Fax: 55-482-319770

Fone: 55-482 / 31-9643

Abstract - This paper presents an accurate and explicit MOSFET model valid in all regions of operation. Physical properties are carefully observed in order to achieve a proper prediction of device behavior. The surface potential is formulated as a function of terminal voltages which, in conjunction with Brews model, results in an explicit MOSFET model.

1 - Introduction

The MOS technology has proven to be well suited for the implementation of mixed analog-digital systems. The validation of analog design by simulation depends upon the precision and computational efficiency of MOSFET models.

Analytical MOSFET models valid in all regions of operation have been developed in which the MOSFET characteristics are expressed in terms of surface potentials at source and drain channel ends [1]. To obtain these potentials one should solve an implicit equation by an iterative procedure [1]. The complexity and waste of time thus involved prevent such models from being applied in computer aided design programs.

In turn, CAD models based on the usual linear dependence of the inversion layer charge on the gate voltage do not describe adequately the MOSFET behavior [2, 3], mainly in the so-called "moderate" inversion region. These models fail in predicting specific requirements of analog circuits design such as small-signal parameters and large signal nonlinearities. Otherwise, semiempirical MOSFET models require the introduction of several empirical parameters [4, 5].

In this paper we derive a very accurate explicit relationship for the surface potential (section III) based on a precise model of the semiconductor capacitance per unit area (section II). The characteristics of the intrinsic long-channel MOSFET in terms of surface potentials at source and drain ends are revised in sections IV and V. Concluding remarks are given in section VI.

II - Approximation of the Semiconductor Capacitance

The expressions that follow are related to the n-channel MOS transistor.

The model presented in this paper is based on an explicit formulation of the semiconductor capacitance per unit area, C_c' , at inversion. This capacitance is a function of the surface potential ϕ_s , according to the following expression [1]:

$$C_c' = \frac{C_{ox}'\gamma}{2} \frac{1 + e^{(\phi_s - 2\phi_f - V_{CB})/\phi_t}}{\sqrt{\phi_s + \phi_f e^{(\phi_s - 2\phi_f - V_{CB})/\phi_t}}} \quad (1)$$

where V_{CB} is the quasi Fermi potential of the minority carriers, ϕ_t is the thermal voltage, ϕ_f is the Fermi potential, C_{ox}' is the oxide capacitance per unit area and γ is the body effect factor.

The semiconductor charge density Q_c' and the depletion charge density Q_B' are given by [1]

$$Q_c' = -C_{ox}'\gamma\sqrt{\phi_s + \phi_f e^{(\phi_s - 2\phi_f - V_{CB})/\phi_t}} \quad (2.a)$$

$$Q_B' = -C_{ox}'\gamma\sqrt{\phi_s} \quad (2.b)$$

Substituting eqns (2) into eqn (1), one obtains

$$C_c' = \frac{Q_c'^2 - Q_B'^2 + 2\phi_t\gamma^2 C_{ox}'^2}{2\phi_t|Q_c'|} \quad (3)$$

According to the charge-sheet approximation, Q_c' - Q_B' is the inversion layer charge density Q_i' . C_c' is, thus, expressed by the compact formula

$$C_c' = \frac{|Q_i'|}{2\phi_t} \left(1 + \frac{Q_B'}{Q_c'} \right) + \frac{C_{ox}'^2\gamma^2}{2|Q_c'|} \quad (4)$$

where the first and second terms represent C_i' and C_b' , the inversion and depletion capacitances per unit area, respectively.

From (4), according to physical behavior, C_i' tends to $|Q_i|/(2\phi_1)$ at very strong inversion, since Q_C' is much greater than Q_B' . Otherwise, C_i' is almost equal to $|Q_i|/\phi_1$ in weak inversion.

A widely used linear approximation of the inversion charge density at strong inversion is

$$Q_i' = -C_{ox}' (V_{GB} - V_T), \quad (5.a)$$

where V_{GB} is the gate-bulk voltage, V_T is the threshold voltage given by

$$V_T = V_{FB} + \phi_M + \gamma \sqrt{\phi_M} \quad (5.b),$$

and $\phi_M = 2\phi_F + V_{CB}$. Fig.1 shows that eqn.(5.a) leads to a significant overestimation of the inversion charge, even for high gate voltages. In order to compensate for this overestimation, we have neglected Q_B'/Q_C' in eqn.(4). Furthermore, we have approximated the term corresponding to the depletion capacitance per unit area by its value at threshold:

$$C_b' = C_b'(\phi_M) = \frac{C_{ox}' \gamma}{2\sqrt{\phi_M}}, \quad (6)$$

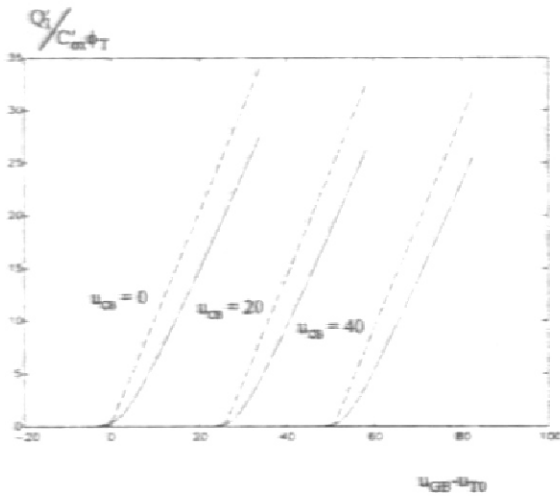


Fig.1. Normalized Inversion Charge Density
 — Numerical expression [1]
 - - - Expression (5)

$$u_{CB} = \frac{V_{GB}}{\phi_1}; \quad u_{CB} = \frac{V_{CB}}{\phi_1}; \quad u_{T0} = \frac{V_T}{\phi_1} \text{ for } V_{CB}=0$$

$$N_A = 2 \times 10^{16} \text{ cm}^{-3}; \quad \mu_n = 250 \text{ A}; \quad V_{FB} = -0.86 \text{ V}$$

An explicit and very simple formula of C_c' is thus obtained:

$$C_c' = C_{ox}' \frac{(V_{GB} - V_T)}{2\phi_T} + (n-1)C_{ox}' \quad \text{for } V_{GB} \geq V_T \quad (7)$$

$$\text{where } n = 1 + \frac{C_b'(\phi_M)}{C_{ox}'} = 1 + \frac{\gamma}{2\sqrt{\phi_M}} \quad (8)$$

Expression (7) is an improved version of an accurate model derived in [6] that allows to determine the harmonic distortion in MOS gate capacitors at strong inversion.

Fig.2 shows that eqn.(7) is very precise at least up to $C_c' = 10C_{ox}'$. The precision in the approximation of eqn.(7), for values of C_c' greater than $10C_{ox}'$ has little effect in the accurate determination of the surface potential (section III).

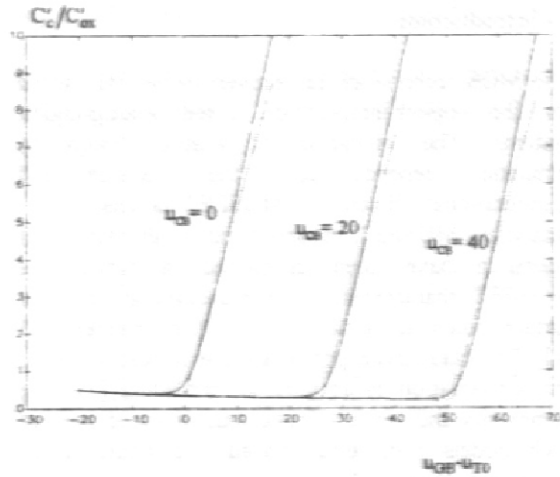


Fig.2. Normalized Semiconductor Capacitance per Unit Area
 — Numerical expression [1]
 - - - Expression (7) with depletion approximation
 for $V_{GB} < V_T$

$$u_{CB} = \frac{V_{GB}}{\phi_1}; \quad u_{CB} = \frac{V_{CB}}{\phi_1}; \quad u_{T0} = \frac{V_T}{\phi_1} \text{ for } V_{CB}=0$$

III - Explicit Formulation of the Surface Potential

Since

$$\frac{\partial \phi_S}{\partial V_{GB}} = \frac{1}{1 + C_c' / C_{ox}'}, \quad (9)$$

the surface potential, for $V_{GB} \geq V_T$, is

$$\phi_S = \phi_M + \int_{V_T}^{V_{GB}} \frac{dV_{GB}}{1 + C'_c/C'_{ox}} \quad (10)$$

Substituting eqn.(7) into eqn.(10), we find that

$$\phi_S = \phi_M + 2\phi_t \ln \left(1 + \frac{V_{GB} - V_T}{2n\phi_t} \right) \quad \text{for } V_{GB} \geq V_T \quad (11)$$

with the important features:

$$\frac{\partial \phi_S}{\partial V_{GB}} = \frac{1}{n} \quad \text{and} \quad \frac{\partial \phi_S}{\partial V_{CB}} = 0 \quad \text{at } V_{GB} = V_T \quad (12)$$

In weak inversion the classical expression of the surface potential

$$\phi_S = 2\phi_F + V_P \quad \text{for } V_{GB} \leq V_T \quad (13.a)$$

has been used in this paper.

Here, V_P is the pinch-off voltage [7], defined as the value of V_{CB} at which the transistor is in the limit of weak inversion for a given V_{GB} .

$$V_P = \left(\sqrt{V_{GB} - V_{FB} + \frac{\gamma^2}{4}} - \frac{\gamma}{2} \right)^2 - 2\phi_F \quad (13.b)$$

Eqs.(11) and (13) provide a continuous transition from weak to strong inversion as well as from conduction to saturation for both ϕ_S (fig.3) and its first order derivatives.

By taking into account that $\frac{\partial V_T}{\partial V_{CB}} = n$, the expressions below are obtained for the derivatives of ϕ_S with respect to V_{GB} and V_{CB} .
For $V_{GB} \leq V_T$:

$$\frac{\partial \phi_S}{\partial V_{GB}} = \frac{1}{1 + \frac{\gamma}{2\sqrt{2\phi_F + V_P}}} \quad (14.a)$$

$$\frac{\partial \phi_S}{\partial V_{CB}} = 0 \quad (14.b)$$

For $V_{GB} \geq V_T$:

$$\frac{\partial \phi_S}{\partial V_{GB}} = \frac{1}{n \left(1 + \frac{V_{GB} - V_T}{2n\phi_t} \right)} \quad (14.c)$$

$$\frac{\partial \phi_S}{\partial V_{CB}} = 1 - n \left(1 - \frac{V_{GB} - V_T}{n^2} - \frac{\gamma}{4\phi_M^{3/2}} \right) \frac{\partial \phi_S}{\partial V_{GB}} \quad (14.d)$$

In refs.[1], [8] and [9] the DC and AC parameters are computed in terms of the surface potentials at source and drain ends and their derivatives. Therefore, eqns.(11), (13) and (14) allow us to evaluate the transistor parameters in an explicit form (sections IV and V).

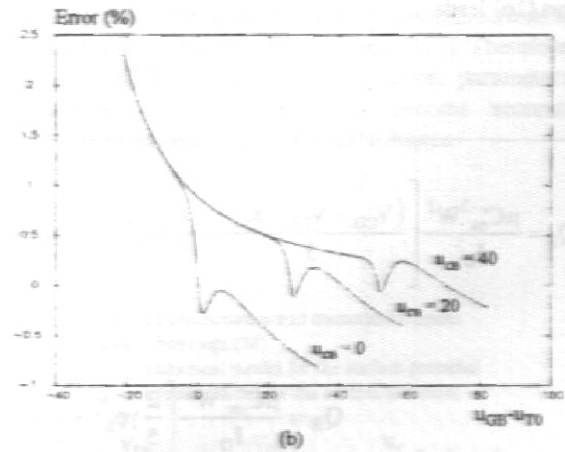
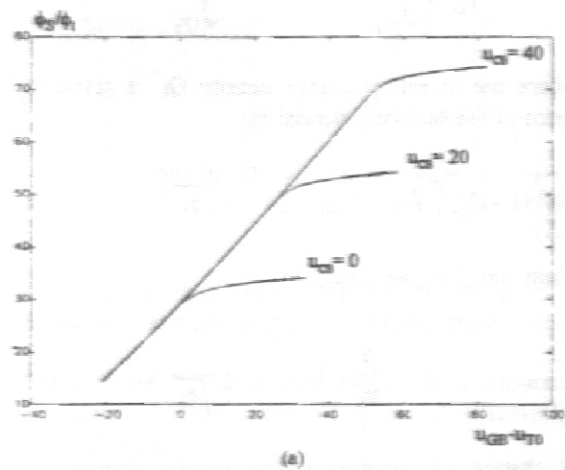


Fig.3. (a) Normalized surface potential
— numerical expression [1]
..... expressions (11) and (13)
(b) Percentual error in computing ϕ_S from eqns. (11) and (13)

$$u_{GB} = \frac{V_{GB}}{\phi_t}; \quad u_{CB} = \frac{V_{CB}}{\phi_t}; \quad u_{T0} = \frac{V_T}{\phi_t} \quad \text{for } V_{CB} = 0$$

IV - Drain Current and Total Charges

According to [1] the drain current is given by

$$I_D = \mu C_{ox} \frac{W}{L} \left[(V_{GB} - V_{FB}) \phi_S - \frac{1}{2} \phi_S^2 - \frac{2}{3} \gamma \phi_S^{3/2} + \phi_t (\phi_S + \gamma \sqrt{\phi_S}) \right]_{\phi_{s0}}^{\phi_{sL}} \quad (15)$$

where ϕ_{s0} and ϕ_{sL} are the surface potentials at source and drain, respectively, μ is the carrier mobility, W is the channel width and L is the channel length.

For a general charge sheet model, the total inversion layer charge Q_I is calculated in [1] from

$$Q_I = \frac{\mu W^2}{I_D} \left[\int_{\phi_{s0}}^{\phi_{sL}} (-Q_i'^2) d\phi_S + \int_{Q_{is}}^{Q_{id}} Q_i' \phi_t dQ_i' \right] \quad (16)$$

where the inversion charge density Q_i' is given in terms of the surface potential by

$$Q_i' = -C_{ox}' (V_{GB} - V_{FB} - \phi_S - \gamma \sqrt{\phi_S}) \quad (17)$$

From eqn.(17), we obtain

$$\frac{\partial Q_i'}{\partial \phi_S} = C_{ox}' \left(1 + \frac{\gamma}{2\sqrt{\phi_S}} \right) \quad (18)$$

A change of variable in the second integral of eqn.(16) leads to

$$Q_I = \frac{\mu C_{ox}'^2 W^2}{I_D} \left[\frac{(V_{GB} - V_{FB} - \phi_S)^3}{3} - \frac{4}{5} \gamma \phi_S^{5/2} - \frac{\gamma^2}{2} \phi_S^2 + \frac{4}{3} (V_{GB} - V_{FB}) \gamma \phi_S^{3/2} - \phi_t \frac{(V_{GB} - V_{FB} - \phi_S - \gamma \sqrt{\phi_S})^2}{2} \right]_{\phi_{s0}}^{\phi_{sL}} \quad (22)$$

$$Q_B = \frac{\mu C_{ox}'^2 W^2}{I_D} \left[\frac{2}{5} \gamma \phi_S^{5/2} + \frac{\gamma}{2} \phi_S^2 - \frac{2}{3} \gamma (V_{GB} - V_{FB} + \phi_t) \phi_S^{3/2} - \frac{\gamma^2}{2} \phi_t \phi_S \right]_{\phi_{s0}}^{\phi_{sL}} \quad (23)$$

$$Q_I = -\frac{\mu W^2}{I_D} \int_{\phi_{s0}}^{\phi_{sL}} \left[Q_i'^2 - Q_i' C_{ox}' \phi_t \left(1 + \frac{\gamma}{2\sqrt{\phi_S}} \right) \right] d\phi_S \quad (19)$$

Similarly, the total depletion charge Q_B can be evaluated from

$$Q_B = \frac{\mu W^2}{I_D} \left[\int_{\phi_{s0}}^{\phi_{sL}} (-Q_i' Q_B') d\phi_S + \int_{Q_{Bs}}^{Q_{Bd}} Q_B' \phi_t dQ_B' \right] \quad (20)$$

which becomes, after a change of variable in the second integral,

$$Q_B = -\frac{\mu W^2}{I_D} \int_{\phi_{s0}}^{\phi_{sL}} \left[Q_B' Q_i' - Q_B' C_{ox}' \phi_t \left(1 + \frac{\gamma}{2\sqrt{\phi_S}} \right) \right] d\phi_S \quad (21)$$

Solving the integrals in eqns.(19) and (21), the following expressions for Q_I and Q_B in terms of surface potentials at source and drain ends of the channel are obtained:

The substitution of eqns.(11) and (13) into eqns. (15), (22) and (23) allows us to express the drain current (fig.4) and the total charges as explicit functions of terminal voltages.

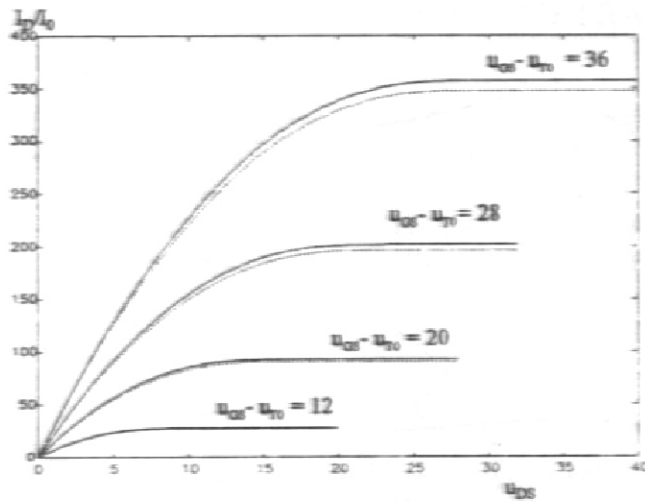


Fig. 4. Normalized Drain Current
 — surface potential computed numerically [1]
 - - - surface potential computed from eqns.(11) and (13)

$$u_{DS} = \frac{V_{DS}}{\phi_1}; \quad u_{GS} = \frac{V_{GS}}{\phi_1}; \quad u_{T0} = \frac{V_T}{\phi_1} \text{ for } V_{CS}=0; \quad I_0 = \frac{W}{L} \mu C_{ox} \phi_1^2$$

V - Small Signal Parameters

According to [1], the gate and bulk transconductances, g_m and g_{mb} , and the drain conductance, g_d , are calculated by differentiating eqn.(15). The following results are obtained:

$$g_m = \mu \frac{W}{L} \left[C_{ox} (\phi_{SL} - \phi_{S0}) + \frac{\partial \phi_{SL}}{\partial V_{GS}} Q_X(\phi_{SL}) - \frac{\partial \phi_{S0}}{\partial V_{GS}} Q_X(\phi_{S0}) \right] \quad (24.a)$$

$$g_{mb} = \mu \frac{W}{L} \left[C_{ox} (\phi_{S0} - \phi_{SL}) + \frac{\partial \phi_{SL}}{\partial V_{BS}} Q_X(\phi_{SL}) - \frac{\partial \phi_{S0}}{\partial V_{BS}} Q_X(\phi_{S0}) \right] \quad (24.b)$$

$$g_d = \mu \frac{W}{L} \frac{\partial \phi_{SL}}{\partial V_{DS}} Q_X(\phi_{SL}) \quad (24.c)$$

$$\text{where } Q_X(\phi_s) = Q_s(\phi_s) + C_{ox} \phi_T \left(1 + \frac{\gamma}{2\sqrt{\phi_s}} \right) \quad (25)$$

and V_{GS} , V_{BS} , and V_{DS} are the gate-to-source, bulk-to-source and drain-to-source voltages, respectively.

The MOSFET intrinsic capacitances for quasi-static operation [1] are determined by differentiating eqns.(22) and (23).

ϕ_{S0} , ϕ_{SL} and their derivatives are explicit functions of the terminal voltages (eqns.(11) and (13)). Therefore, all the MOSFET intrinsic small signal parameters, illustrated in figs.(5) and (6), become accurate explicit functions of the terminal voltages.

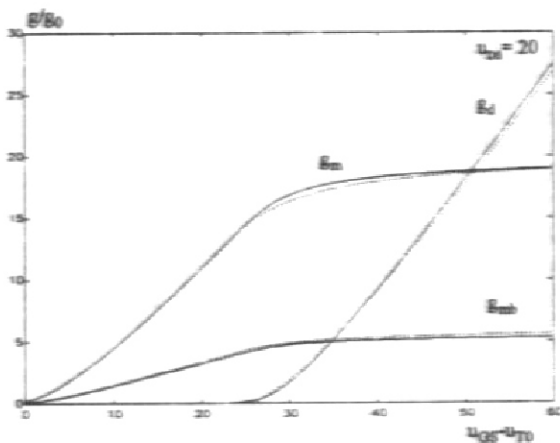


Fig. 5. Normalized conductance and transconductances calculated from eqn.(24)
 — numerical model for the surface potential
 - - - explicit model for the surface potential

$$u_{DS} = \frac{V_{DS}}{\phi_1}; \quad u_{GS} = \frac{V_{GS}}{\phi_1}; \quad u_{T0} = \frac{V_T}{\phi_1} \text{ for } V_{CS}=0;$$

$$g_0 = \frac{W}{L} \mu C_{ox} \phi_1$$

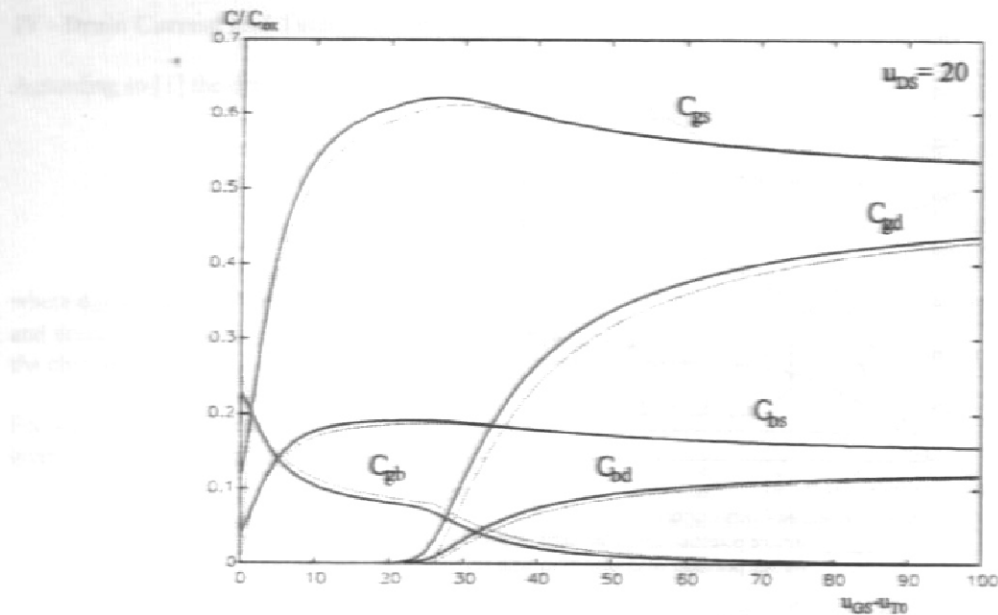


Fig. 6. Normalized intrinsic capacitances

— numerical model for the surface potential
 explicit model for the surface potential

$$u_{DS} = \frac{V_{DS}}{\phi_1} \quad u_{GS} = \frac{V_{GS}}{\phi_1} \quad u_{T0} = \frac{V_T}{\phi_1} \text{ for } V_{CB}=0$$

VI - Conclusions

We have accomplished a general explicit model appropriate for the simulation of MOSFET circuits. The formulation has an excellent accuracy in moderate inversion since the approximation of the semiconductor capacitance is precise around threshold. Thus, a smooth variation of device characteristics is guaranteed through the entire inversion region.

REFERENCES

- [1] Y. Tsividis, "Operation and modeling of the MOS transistor", McGraw-Hill, New York, 1987.
- [2] Y. Tsividis and G. Masetti, "Problems in precision modeling of the MOS transistor for analog applications", IEEE Trans. on CAD, vol. CAD-3, pp. 72-79, January 1984.
- [3] C. Turchetti and G. Masetti, "A CAD-oriented analytical MOSFET model for high-accuracy applications", IEEE Trans. on CAD, vol. CAD-3, pp. 117-122, April 1984.
- [4] B. Iñiguez and E.G. Moreno, "Explicit C_{sc} -continuous and general model for n MOSFETs", Electronics Letters, vol.29, pp.1036-1037, May 1993.
- [5] C. Enz, "High-precision CMOS micropower amplifiers", Ph-D Thesis, EPF-Lausanne, 1989.
- [6] A.T. Behr, M. C. Schneider, S. Noceti Filho and C.G. Montoro, "On the harmonic distortion caused by capacitors implemented with MOSFET gates", IEEE J. Solid-State Circuits, vol. SC27, pp. 1470-1475, October 1992.
- [7] E. Vittoz, "Intensive Summer Course on CMOS VLSI Design - Analog & Digital", EPF-Lausanne, 1989.
- [8] C. Turchetti, G. Masetti and Y. Tsividis, "On the small-signal behaviour of the MOS transistor in quasistatic operation", Solid-State Electronics, vol.26, N° 10, pp. 941-949, 1983.
- [9] M. Bagheri and Y. Tsividis, "A small signal dc-to-high-frequency nonquasistatic model for the four-terminal MOSFET valid in all regions of operation", IEEE Trans on Electron. Devices, vol. ED-32, pp.2383-2391, November 1985.